ISOGEOMETRIC FREE VIBRATION OF AN ELASTIC BLOCK

Radek Kolman*

Modification of the Finite Element Method (FEM) based on the different types of spline shape functions is an up-to-date strategy for numerical solution of partial differential equations (PDEs). This approach has an advantage that the geometry in Computer Graphics framework and approximation of fields of unknown quantities in FEM are described by the same technique. The spline variant of FEM is often called the Isogeometric Analysis (IGA). Another benefit of this numerical solution of PDEs is that the approximation of unknown quantities is smooth. It is an outcome of higher-order continuity of spline basis functions. It was shown, that IGA produces outstanding convergence rate and also appropriate frequency errors. Polynomial spline (C^{p-1} continuous piecewise polynomials, $p \geq 2$) shape functions produce low dispersion errors and moreover, dispersion spectrum of unbounded domains does not include optical modes unlike FEM based on the higher-order C^0 continuous Lagrange interpolation polynomials. In this contribution, the B-spline (NURBS with uniform weights) shape functions in the FEM framework are tested in the numerical solution of free vibration of an elastic block. The main attention is paid to the comparison of convergence rate and accuracy of IGA with the classical Lagrangian FEM, Ritz method and experimental data.

Keywords: *isogeometric analysis, finite element method, B-spline and NURBS basis functions, free vibration, eigen-value problem, resonant ultrasound spectroscopy*

1. Introduction

A modern approach in computational continuum mechanics is Isogeometric Analysis (IGA). This modification of Finite Element Method (FEM) employs shape functions based on different types of splines (B-splines, NURBS, T-splines and many others). A lot of two- and three-dimensional geometries could be described by NURBS (Non-Uniform Rational B-spline) representation exactly, as conic section-like surfaces. For details of IGA concept see the book [1]. Isogeometric analysis aims to integrate finite element (FE) ideas in commercial Computer Aided Design (CAD) systems without necessity to generate new computational meshes. IGA concept was successfully employed for numerical solutions of different physical and mathematical problems, as fluid dynamics, diffusion and heat problems or continuum mechanics, etc. It was shown, that IGA produces optimal convergence rate and dispersion properties in elastodynamics and also appropriate eigen-frequency errors [2, 3]. In addition, this approach provides higher degree of continuity than that offered by the classical FEM based on Lagrange polynomials. In mathematics, a spline is defined as a sufficiently smooth piecewise-polynomial function. Generally, a lot of spline types exist [4]. It is commonly accepted that the first mathematical reference to splines is the 1946 paper by Schoenberg [5],

* Ing. R. Kolman, Ph.D., Institute of Thermomechanics AS CR, v. v. i., Dolejškova 5, 182 00 Praha 8

which is probably the first place where the word 'spline' is used in connection with smooth, piecewise polynomial approximation.

In this paper, the IGA concept will be shortly described and applied to the computation of eigen-frequencies of an elastic prismatic block. This benchmark is the ideal test for the verification and validation of an in-house implemented IGA code. The efficiency, accuracy and convergence properties of the IGA eigen-frequency computation will be compared with classical FEM, Ritz method and also experimental data. Geometry and material parameters of eigen-vibration problem of an elastic block is taken over from the paper [6].

The second motivation is to apply the IGA strategy in the resonant ultrasound spectroscopy (RUS). RUS method was developed for the determination of elastic moduli of generally anisotropic materials, especially those of single crystals [7, 8]. In the RUS technology, complex amplitudes of the forced harmonic vibration and natural frequencies are identified for a particular specimen. Provided a sufficient number of frequencies were accurately measured and given mass density, dimensions, the shape of the specimen and the type of material symmetry, all elastic moduli can be determined in a single experiment.

Generally, resonance (eigen) frequencies are calculated from a mathematical model of the free vibration of an elastic body with stress–free boundaries. Frequently, the Rayleigh-Ritz method [9] is widely used for the calculation of the natural vibration frequency of structures [10]. It is a direct variational method in which the minimum of a functional defined on a normed linear space is approximated by a linear combination of elements from that space. Practically, this method is based on a choice of shape, basis functions satisfying boundary conditions. In this case, there are stress–free boundary conditions.

Troubles with a choice of basis functions for the Rayleigh-Ritz method could arise for an arbitrary geometry of specimens. For example, shape functions satisfying stress–free boundary conditions have been found for sphere, cube, cylinder, ellipsoid and more other simple bodies, see [7, 8]. A pioneering numerical algorithm based on the Rayleigh-Ritz method using trigonometric functions for cubic specimens was proposed by Holland [11]. Its convergence was later improved introducing Legendre's polynomials by Demarest [12]. Ohno [13] extended the Demarest's solution to parallelepiped rectangle with orthorhombic symmetry. Visscher et al. [15] proposed a simple computational scheme for the free vibration of a specimen with anisotropic properties using basis functions in the form $x^l\, y^m\, z^n$. This algorithm is known as the *xyz algorithm* and the method is applicable even for various irregularly-shaped bodies composed of anisotropic media. The *xyz algorithm* will be exploited for comparison with the IGA computation.

Using the Rayleigh-Ritz method for the solution of the governing eigen-problem is limited to specimens of simple shapes as blocks, spheres, cylinders, etc. Instead, FEM and IGA can be employed [6, 14] for arbitrary bodies made of heterogeneous, anisotropic materials. On the other hand, smoothness of eigen-modes on boundary of specimens obtained by IGA technology could be effectively and simply utilized for the inverse determination of material parameters or orientation of crystals and alloys.

In Section 2, foundations of Isogeometric Analysis is presented. The basic equations of eigen-vibration are mentioned in Section 3. The paper closes by the numerical test – eigen-vibration of an elastic block (Section 4) and discussion of accuracy and convergence rates of different numerical strategies (Section 5).

2. Isogeometric analysis – spline based FEM

In this section, the basis of spline based FEM will be shortly introduced. The simplest type of spline is a B-spline (basis spline). It is a piecewise polynomial function with higher-order continuity between individual intervals. In CAD, a B-spline curve is given by the linear combination of B-spline basis functions $N_{i,p}$, see book [16],

$$\mathbf{C}(\xi) = \sum_{i=1}^{n} N_{i,p}(\xi)\,\mathbf{P}_i \ , \tag{1}$$

where $\xi \in [\xi_1, \xi_{m_k}] \subset \mathbb{R}$ is the parameter and $\mathbf{P}_i, i = 1, 2, \ldots, n$ are the vectors of coordinates of control points. B-spline basis functions $N_{i,p}(\xi)$ are prescribed by the Cox-de Boor recursion formula, see [16]. For a given knot vector Ξ, $N_{i,p}(\xi)$ are defined recursively starting with piecewise constants ($p = 0$)

$$N_{i,0}(\xi) = \begin{cases} 1 & \text{if} \quad \xi_i \le \xi \le \xi_{i+1} \ , \\ 0 & \text{otherwise} \ . \end{cases} \tag{2}$$

For $p = 1, 2, 3, \ldots$ they are defined by

$$N_{i,p}(\xi) = \frac{\xi - \xi_i}{\xi_{i+p} - \xi_i}\, N_{i,p-1}(\xi) + \frac{\xi_{i+p+1} - \xi}{\xi_{i+p+1} - \xi_{i+1}}\, N_{i+1,p-1}(\xi) \ . \tag{3}$$

The knot vector in one-dimensional case is a non-decreasing set of coordinates in the parametric space, written as $\Xi = \{\xi_1, \xi_2, \ldots, \xi_{m_k}\}$, where $\xi_i \in \mathbb{R}$ is the i-th knot, i is the knot index, $i = 1, 2, \ldots, m_k$, where $m_k = n + p + 1$, p is the polynomial order, and n is the number of basis functions and as well the number of control points. Basic properties of B-spline basis functions are [16]

- a partition of unity, that is, $\sum_{i=1}^{n} N_{i,p}(\xi) = 1 \ \ \forall \xi \in [\xi_1, \xi_{m_k}]$,
- the support of each $N_{i,p}$ is compact and contained in the interval $[\xi_i, \xi_{i+p+1}]$,
- B-spline basis functions $N_{i,p}$ are non-negative: $N_{i,p}(\xi) \ge 0 \ \ \forall \xi \in [\xi_1, \xi_{m_k}]$,
- $N_{i,p}$ are C^{p-k} continuous piecewise polynomials, where k is multiplicity of knot. The continuity can be controlled by the multiplicity of knot in the knot vector Ξ.

The knot vector for an open B-spline curve interpolating end points should be in the form $\Xi = \{a, \ldots, a, \xi_{p+2}, \ldots, \xi_n, b, \ldots, b\}$, where values are usually set as $a = 0$ and $b = 1$. The multiplicity of the first and last knot value is $p + 1$. If the values ξ_{p+1} up to ξ_{n+1} are chosen uniformly, the knot vector Ξ is called uniform, otherwise non-uniform, see [16]. An example of cubic B-spline basis functions is displayed in Fig. 1 and an open cubic B-spline curve interpolating end points with its control polygon is presented in Fig. 2.

B-spline surfaces and solids are described by tensor product [16]. A tensor product B-spline surface of degree p, q is defined by

$$\mathbf{S}(\xi, \eta) = \sum_{i=1}^{n} \sum_{j=1}^{m} N_{i,p}(\xi)\, M_{j,q}(\eta)\, \mathbf{P}_{i,j} \ , \tag{4}$$

where $N_{i,p}(\xi)$, $M_{j,q}(\eta)$ are univariate B-spline functions of order p and q corresponding to knot vectors Ξ and $\mathcal{H}$, respectively. $\mathbf{P}_{i,j}$, $i = 1, \ldots, n, j = 1, \ldots, m$ are vectors of coordinates of control points.

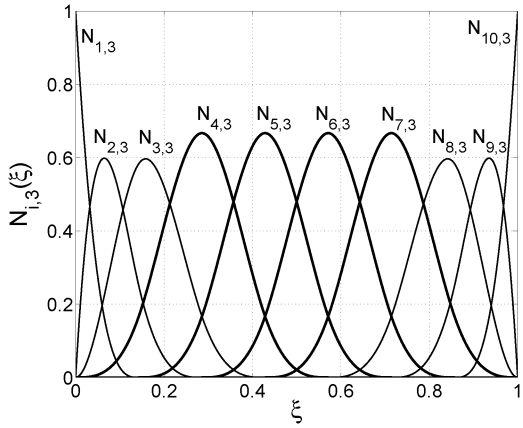

Fig.1: Example of cubic B-spline basis functions for ten control points and the uniform knot vector; thin lines correspond to non-uniform (non-homogeneous) basis functions and thick lines correspond to uniform (homogeneous) basis functions; the number of non-uniform basis functions depends on polynomial order

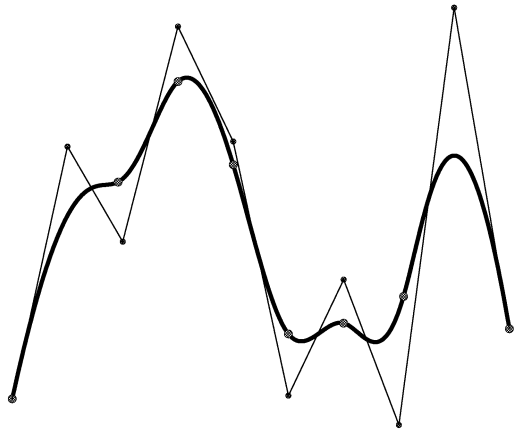

Fig.2: Example of an open cubic B-spline curve interpolating end points for ten control points and the uniform knot vector; the control polygon–piecewise linear interpolation of the control points–is drawn by thin lines; the connecting points (knot points) of piecewise polynomials are shown by white points on the curve

Further, a tensor product B-spline solid of degree p, q, r is expressed by

$$\mathbf{V}(\xi,\eta,\zeta) = \sum_{i=1}^{n}\sum_{j=1}^{m}\sum_{k=1}^{l} N_{i,p}(\xi)\, M_{j,q}(\eta)\, L_{k,r}(\zeta)\, \mathbf{P}_{i,j,k} \ , \tag{5}$$

where $N_{i,p}(\xi)$, $M_{j,q}(\eta)$, $L_{k,r}(\zeta)$ are univariate B-spline functions of order p, q and r corresponding to knot vectors Ξ, $\mathcal{H}$, $\mathcal{Z}$, respectively. $\mathbf{P}_{i,j,k}$, $i = 1,\ldots,n$, $j = 1,\ldots,m$, $k = 1,\ldots,l$ are vectors of coordinates of control points. The main properties of B-spline surface and B-spline solid basis functions are derived from properties of univariate basis functions [16]. A lot of operations with B-spline representation could be made as a knot insertion, order elevation and refinement operation. Therefore h, p, k-refinement is possible to use in the IGA strategy [1].

The step from the B-spline to NURBS is natural, because the NURBS representation can exactly described some domains occurring in engineering design [1]. A NURBS curve of degree p is defined similarly as a B-spline curve by the relationship

$$\mathbf{C}(\xi) = \sum_{i=1}^{n} R_i^p(\xi)\,\mathbf{P}_i \ , \tag{6}$$

where the difference is only in the rational basis functions given by

$$R_i^p(\xi) = \frac{N_{i,p}(\xi)\,w_i}{\sum_{\hat{i}=1}^{n} N_{\hat{i},p}(\xi)\,w_{\hat{i}}} \tag{7}$$

and w_i is referred to as the i-th *weight* corresponding to the i-th control point. For NURBS surfaces and solids, the shape functions are described by the tensor product. It holds

$$R_{i,j}^{p,q}(\xi,\eta) = \frac{N_{i,p}(\xi)\,M_{j,q}(\eta)\,w_{i,j}}{\sum_{\hat{i}=1}^{n}\sum_{\hat{j}=1}^{m} N_{\hat{i},p}(\xi)\,M_{\hat{j},q}(\eta)\,w_{\hat{i},\hat{j}}} \tag{8}$$

and

$$R_{i,j,k}^{p,q,r}(\xi,\eta,\zeta) = \frac{N_{i,p}(\xi)\,M_{j,q}(\eta)\,L_{k,r}(\zeta)\,w_{i,j,k}}{\sum_{\hat{i}=1}^{n}\sum_{\hat{j}=1}^{m}\sum_{\hat{k}=1}^{l} N_{\hat{i},p}(\xi)\,M_{\hat{j},q}(\eta)\,L_{\hat{k},r}(\zeta)\,w_{\hat{i},\hat{j},\hat{k}}} \ , \tag{9}$$

respectively. For details regarding NURBS representation and its main properties see [16].

In IGA, the approximation of a displacement field $\mathbf{u}^h(\mathbf{x})$ is given by the same relationship as the mathematical representation of geometry (by equations $(1), (4), (5)$ or with help of NURBS basis functions $(7), (8), (9)$). For three-dimensional problems it leads to

$$\mathbf{u}^h(\mathbf{x}(\xi,\eta,\zeta)) = \mathbf{u}^h(\xi,\eta,\zeta) = \sum_{i=1}^{n}\sum_{j=1}^{m}\sum_{k=1}^{l} R_{i,j,k}^{p,q,r}(\xi,\eta,\zeta)\,\mathbf{u}_{i,j,k}^{\mathrm{P}} \ , \tag{10}$$

where $\mathbf{u}_{i,j,k}^{\mathrm{P}}$ is the vector of control variables–displacements corresponding to the control point marked by index values i, j, k. In the process, vectors $\mathbf{u}_{i,j,k}^{\mathrm{P}}$, $i = 1, \ldots, n$, $j = 1, \ldots, m$, $k = 1, \ldots, l$ are unknowns of solved problem.

3. Formulation of free vibration of an elastic body

In this section, the strong, weak and matrix formulations of eigen-vibration of an elastic body will be mentioned. For details see books [17, 18, 19].

3.1. Strong formulation

The strong formulation of free vibration problem of a three-dimensional elastic body, occupying a domain $\Omega \subset \mathbb{R}^3$, without constraints is given

$$\sigma_{ij,j} - \rho\,\ddot{u}_i = 0 \quad \text{in} \quad \Omega \times (0,T) \ , \tag{11}$$

$$\sigma_{ij}\,n_j = 0 \quad \text{on} \quad \partial\Omega \times (0,T) \ , \tag{12}$$

where the summation convention has been used. A comma placed before subscripts refers to spatial differentiation whereas the superimposed dots denote the time derivatives. The first

equation has a meaning of the equation of motion and the second one prescribes stress–free boundary conditions. Here, σ_{ij} is the Cauchy stress tensor, u_i is the component of displacement vector $\mathbf{u}(\mathbf{x},t)$, $\mathbf{x} \in \Omega$ is the position vector, $t, T \geq 0$ denote the time, ρ denotes the mass density, n_i is the component of the outward normal vector $\mathbf{n}$ on $\partial\Omega$. The Cauchy stress tensor $\boldsymbol{\sigma}$ and displacement vector $\mathbf{u}$ are put together in the linear theory of elasticity by the Cauchy relationship

$$\epsilon_{ij} = \frac{1}{2}\left(u_{i,j} + u_{j,i}\right) \tag{13}$$

and by the Hooke's law in the form

$$\sigma_{ij} = c_{ijkl}\,\epsilon_{kl}\ . \tag{14}$$

In the previous relationship, ϵ_{ij} marks the infinitesimal strain tensor and c_{ijkl} is the four-order elastic tensor. If a homogeneous isotropic elastic material is assumed, the elastic tensor has the form

$$c_{ijkl} = \lambda\,\delta_{ij}\,\delta_{kl} + G\left(\delta_{ik}\,\delta_{jl} + \delta_{il}\,\delta_{jk}\right)\ , \tag{15}$$

where δ_{ij} is the Kronecker delta. λ and μ are the Lamé parameters given by

$$\lambda = \frac{\nu\,E}{(1+\nu)\,(1-2\,\nu)} \qquad \text{and} \qquad G = \frac{E}{2\,(1+\nu)}\ . \tag{16}$$

E prescribes the Young's modulus and ν is the Poisson's ratio. In a general case, the elastic tensor c_{ijkl} includes 21 independent components.

In this paper, we are interested in the modal analysis in which an elastic body vibrates. We obtain natural modes by separation of variables. We assume the time-spatial distribution of a displacement field $\mathbf{u}(\mathbf{x},t)$ to have the form

$$\mathbf{u}(\mathbf{x},t) = \mathbf{u}(\mathbf{x})\,\mathrm{e}^{\mathrm{i}\,\omega\,t}\ , \tag{17}$$

where $\mathbf{u}(\mathbf{x})$ is a function of spatial variable only, $\mathrm{i} = \sqrt{-1}$ and ω is the natural frequency, $f = \omega/(2\pi)$ is the frequency. Thus, the acceleration field obtained by differentiation of (17) twice with respect to the time has to the form

$$\ddot{\mathbf{u}}(\mathbf{x},t) = -\omega^2\,\mathbf{u}(\mathbf{x},t)\ . \tag{18}$$

The both previous relationships (17) and (18) are the main ones for linear vibration problems.

3.2. Weak formulation and Galerkin formulation

At first, we define the trial solution space, denoted by $\mathcal{S}$, as all of the functions $\mathbf{u}$ which have square-integrable derivatives and also satisfied boundary conditions, in this work, stress–free boundary conditions (12). The second collection of functions $\mathbf{w}$, in which we are interested, is called the space of weighting functions denoted by $\mathcal{V}$. These functions, which are square-integrable up to first derivatives, have to satisfy the homogeneous Dirichlet boundary conditions.

Inserting relationships (13), (14) and (18) into (11), multiplying by weighting function $\mathbf{w}$, and integrating by parts with respect to (12) leads to the weak form: Find all eigen-pairs

$\{\mathbf{u}, \lambda\}$, $\mathbf{u} \in \mathcal{S}$ (space of trial solutions), $\lambda = \omega^2 \in \mathbb{R}^+$, such that for all $\mathbf{w} \in \mathcal{V}$ (space of weighting functions)

$$-\omega^2 \, (\mathbf{w}, \rho \, \mathbf{u}) + a(\mathbf{w}, \mathbf{u}) = 0 \ , \tag{19}$$

where the scalar product is given by

$$(\mathbf{w}, \rho \, \mathbf{u}) = \int_{\Omega} \rho \, \mathbf{w} \cdot \mathbf{u} \, \mathrm{d}\Omega \tag{20}$$

and the bilinear form is defined by

$$a \, (\mathbf{w}, \mathbf{u}) = \int_{\Omega} w_{i,j} \, c_{ijkl} \, u_{k,l} \, \mathrm{d}\Omega \ . \tag{21}$$

The eigen-value $\lambda = \omega^2$ could be also determined by the Rayleigh quotient [20], where a displacement field $\mathbf{u}$ satisfying boundary conditions should be found. The Rayleigh quotient is defined for any $\mathbf{u} \in \mathcal{S}$ as follows

$$\omega^2 = \frac{a(\mathbf{u}, \mathbf{u})}{(\mathbf{u}, \rho \, \mathbf{u})} \ . \tag{22}$$

The first eigenfunction minimizes the Rayleigh quotient and the minimum of the Rayleigh quotient is the first eigenvalue.

The continuous Galerkin formulation, the foundation of the standard formulation of FEM, is obtained by restricting to finite-element subspaces $\mathcal{S}^h \subset \mathcal{S}$, $\mathcal{V}^h \subset \mathcal{V}$. Functions $\mathbf{u}$ and $\mathbf{w}$ in (19) will be replaced by the finite dimensional approximations $\mathbf{u}^h$ and $\mathbf{w}^h$. Thus we can write the i-th component of $\mathbf{u}^h \in \mathcal{S}^h$ and of $\mathbf{w}^h \in \mathcal{V}^h$ as

$$u_i^h = \sum_{A=1}^{N} N_A \, d_{iA} \ , \qquad w_i^h = \sum_{B=1}^{N} N_B \, c_{iB} \ . \tag{23}$$

Indexes $A, B = 1, \ldots, N$ identify corresponding global shape functions and also components of global vector of solution with the length $N_{\mathrm{eq}} = \mathit{NDIM} \cdot N$, where *NDIM* is dimension of the problem and N is total number of control points. In IGA, N_A, N_B are NURBS or B-spline basis functions. In classical FEM, N_A, N_B are piecewise Lagrange interpolation polynomials.

The resulting eigen-pairs will contain approximations of both natural modes $\mathbf{u}^h$ and the natural frequencies ω_k^h: Find $\omega^h \in \mathbb{R}^+$ and $\mathbf{u}^h \in \mathcal{S}^h$ such that for all $\mathbf{w}^h \in \mathcal{W}^h$

$$-(\omega^h)^2 \, (\mathbf{w}^h, \rho \, \mathbf{u}^h) + a(\mathbf{w}^h, \mathbf{u}^h) = 0 \ . \tag{24}$$

This statement is called the Galerkin formulation. Of course, the Rayleigh quotient (22) could be used for the numerical solution of eigen-values based on the Galerkin formulation. The mathematical proof of convergence and error estimation have been published in books [20, 21].

3.3. Matrix formulation

Substituting the finite dimensional approximation $\mathbf{w}^h$ and $\mathbf{u}^h$ given by (23) into (24) leads to a matrix eigen-value problem: Find natural frequency $\omega_k^h \in \mathbb{R}^+$ and $\mathbf{d}_k$, $k = 1, \ldots, N_{\mathrm{eq}}$

such that the matrix form is obtained in the form of well-known generalized eigen-value problem

$$\left[\mathbf{K} - (\omega^h)^2\,\mathbf{M}\right]\mathbf{d} = \mathbf{0}\ , \tag{25}$$

where $\mathbf{K}$ and $\mathbf{M}$ is global stiffness and mass matrix, respectively. The solution of the generalized eigen-value problem are the eigen-pairs – eigen-values ω_i^h and the corresponding eigen-vectors $\mathbf{d}_k$, $k = 1, \ldots, N_{\mathrm{eq}}$ [19].

In principle, the eigen-vectors $\mathbf{d}_k$ could be normalized arbitrarily. In practise, the eigen-vectors $\mathbf{d}_k$, $k = 1, \ldots, N_{\mathrm{eq}}$ constituting the modal matrix $\mathbf{V} = [\mathbf{d}_1, \mathbf{d}_2, \ldots, \mathbf{d}_{N_{\mathrm{eq}}}]$ satisfy the relationship

$$\mathbf{V}^{\mathrm{T}}\,\mathbf{M}\,\mathbf{V} = \mathbf{I}\ , \tag{26}$$

where $\mathbf{I}$ is the unit matrix and then with respect to (25) and (26), it holds

$$\mathbf{V}^{\mathrm{T}}\,\mathbf{K}\,\mathbf{V} = \mathbf{\Lambda}\ , \tag{27}$$

where the diagonal matrix $\mathbf{\Lambda}$ denotes the spectral matrix that stores the eigen-values ω_i^h, $\mathbf{\Lambda} = \mathrm{diag}[(\omega_1^h)^2, (\omega_2^h)^2, \ldots, (\omega_{N_{\mathrm{eq}}}^h)^2]$.

Practically, the stiffness matrix $\mathbf{K}$ and mass matrix $\mathbf{M}$ in the IGA strategy are defined by the same relationships as in the standard FEM, see [19]. Remark, linear spline IGA is identical with the standard linear FEM, where hat shape functions are carried out. The stiffness and mass matrices are given by

$$\mathbf{K} = \int_{\Omega} \mathbf{B}^{\mathrm{T}}\,\mathbf{C}\,\mathbf{B}\,\mathrm{d}\Omega\ , \qquad \mathbf{M} = \int_{\Omega} \rho\,\mathbf{N}^{\mathrm{T}}\,\mathbf{N}\,\mathrm{d}\Omega\ , \tag{28}$$

where $\mathbf{C}$ is the elasticity matrix, ρ is the mass density, $\mathbf{B}$ is the strain-displacement matrix, $\mathbf{N}$ stores the displacement shape functions and integration is carried over the non-deformed domain Ω. Global matrices are assembled in the usual fashion. Mass matrix defined by the relationship (28) is called the consistent mass matrix. If the theory of linear elastodynamics is considered, then the mass matrix, $\mathbf{M}$, and the stiffness matrix, $\mathbf{K}$, are constant. These matrices are evaluated by the Gauss-Legendre quadrature formula, see [19]. A lot of numerical methods for solution of eigen-value problem exist [19], but this paper is not devoted to the testing of numerical methods for eigen-value problem.

4. Numerical test – free vibration of an elastic block

In this section, the benchmark test – vibration of an elastic block will be defined and numerically solved for different spatial discretizations.

4.1. Formulation of the problem

The geometrical parameters of a rectangular glass block, their elastic and mass properties are adopted from the work [6]. The specimen has the rectangular block form with dimensions 2.333×2.889×3.914 mm. Material's elastic moduli $\bar{C}_{11} = 82.0407$, $\bar{C}_{12} = 23.5666$ and $\bar{C}_{44} = 29.2371$ in GPa were identified by the pulse method [22]. Maximum error of the measurement was estimated to 1.3 % and, therefore, the ranges of the elastic moduli were $C_{11} \in (80.97, 83.11)$, $C_{12} \in (23.26, 23.87)$ and $C_{44} \in (28.86, 29.62)$. Glass is an isotropic material, thus, $C_{44} = (C_{11} - C_{12})/2$. For simulation purposes, the moduli C_{11}, C_{12} and C_{44}

were understood as independent, that is, cubic symmetry of elastic tensor was assumed. Mass density $\rho = 2459.9\,\mathrm{kg/m^3}$ was determined by weighing in the water, for details see [6].

The eigen-frequencies of the specimen were determined by the RUS method with the absolute error 105 Hz. Hence, the relative error is 10^{-4}. The first twenty non-zero eigen-frequencies $f_i = \omega_i/(2\pi)$, $i = 1, 2, \ldots, 20$ are presented in [6] and also at the last column of Tab. 1.

Freq. no.	Ritz method[a] $x^l y^m z^n$ [6]	FEM[b] linear [6]	FEM[b] quadr. serend. [6]	IGA[c] $p=2$ NP	IGA[c] $p=2$ LP	IGA[c] $p=3$ NP	IGA[c] $p=3$ LP	'Refer.' result[d] [6]	Exper. data [6]
1	389154	390170	389158	390229	389192	389719	389143	389140	390195
2	483641	485224	483680	484405	483756	484094	483641	483639	482385
3	523541	525046	523580	524444	523654	524065	523541	523540	521235
4	643221	644500	643253	644381	643328	643770	643218	643216	640560
5	669073	669420	669079	669711	669088	669346	669073	669074	664640
6	684101	686523	684109	686157	684196	685197	684068	684061	684450
7	714654	717079	714716	715894	714873	715267	714648	714642	712135
8	723969	727324	723784	726522	723928	725292	723718	723705	723825
9	742704	744788	742760	744294	742881	743613	742697	742695	741780
10	805803	808032	805840	807347	805930	806649	805791	805789	803200
11	813858	816768	813875	815119	813931	814471	813844	813843	809640
12	829406	831475	829346	831343	829466	830332	829292	829286	825390
13	831333	833803	831275	833022	831372	832224	831226	831221	831760
14	856984	860732	856580	860164	856798	858498	856489	856469	854790
15	912615	913178	912624	913542	912640	913011	912615	912615	906720
16	968242	971463	968386	971842	968694	970094	968270	968248	964085
17	1000636	1007520	1000800	1003989	1001143	1002303	1000656	1000640	1004090
18	1007289	1010840	1007390	1010058	1007604	1008749	1007293	1007280	1020470
19	1023977	1028970	1024160	1027299	1024571	1026041	1023999	1023970	1024880
20	1026657	1032200	1026770	1031071	1027043	1029187	1026660	1026630	1033700

NP – non-linear parameterization
LP – linear parameterization
a – order $p = 10$
b – FE mesh density 10×10×10
c – number of control points 10×10×10
d – FE mesh density 20×20×20

Tab.1: The first twenty non-zero eigen-frequencies of a glass block in Hz computed by IGA, FEM, Ritz method and compared with experimental data [6]

4.2. Comparison of accuracy and convergence rates

The IGA, FEM and Ritz method are tested in eigen-vibration of a glass specimen of a block form described in the previous section. FEM computations are realized by FE program PMD [23]. Linear and quadratic serendipity FE meshes were employed [19]. In the Ritz method, the *xyz algorithm* implemented in program RPR [24] is used with different order of polynomials (ten up to twelve). The IGA code was implemented in Matlab environment [27].

For the IGA concept, the block is discretized by linear ($p = 1$), quadratic ($p = 2$) and cubic ($p = 3$) B-splines for different number of control points. The block with straight boundary can be exactly described by the B-spline representation using NURBS. It is by NURBS representation with uniform weights of control points. The uniform knot vectors are used in all parametric directions, but two types of parameterizations are tested. The first

of them is the non-linear parameterization given by uniformly-spaced control points. The second parameterization is described by the Greville abscissa [25], where positions of control points are uniquely given by the averaged knot vector components

$$x_i^* = \frac{\xi_{i+1} + \cdots + \xi_{i+p}}{p} \ , \quad i = 1, 2, \ldots, n \ . \tag{29}$$

In such a case, the abscissa is associated with the knot vector Ξ. If the knot vector is chosen so that $a = 0$, $b = 1$ in the knot vector and the end knots have $p + 1$ multiplicity, then the boundary control points are located on $x_1^* = 0$ and $x_n^* = 1$. B-spline representation with the Greville abscissa is passed through end points. Therefore, the coordinates x_i, y_j, z_k of control points of a B-spline solid with dimensions $h_x \times h_y \times h_z$ are given by

$$x_i = x_i^* \cdot h_{\mathrm{x}} \ , \qquad y_j = y_j^* \cdot h_{\mathrm{y}} \ , \qquad z_k = z_k^* \cdot h_{\mathrm{z}} \ . \tag{30}$$

This parameterization is then linear. It means that the mapping for the parametric space to the geometrical one is linear and Jacobian of this transformation is a constant value [3]. This linear parameterization produces smaller dispersion and frequency errors then the uniform one [26]. On the other hand, the higher-order spline discretization with linear parameterization shows 'outlier frequencies' but with smaller frequency errors than the non-linear parameterization [3]. The 'outlier frequencies' correspond to the vibration of boundary ranges of a domain. In the Fig. 3, the comparison of non-linear parameterization of a block and linear parameterization given by the Greville abscissa is shown.

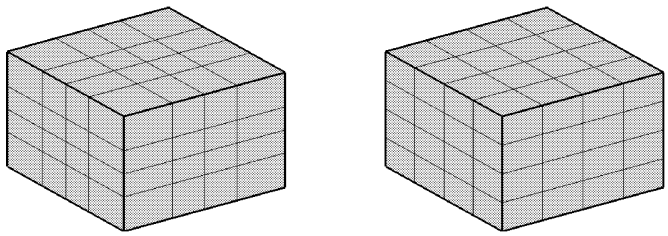

Fig.3: Comparison of non-linear parameterization of a block (on the left) and linear parameterization (on the right) given by the Greville abscissa [25]; thin lines are knot parametric lines

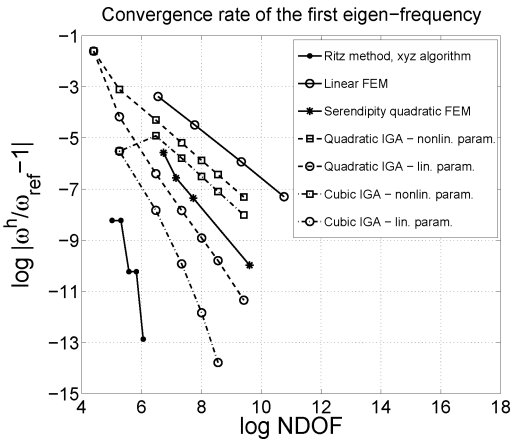

Fig.4: Convergence rates for the first non-zero frequency

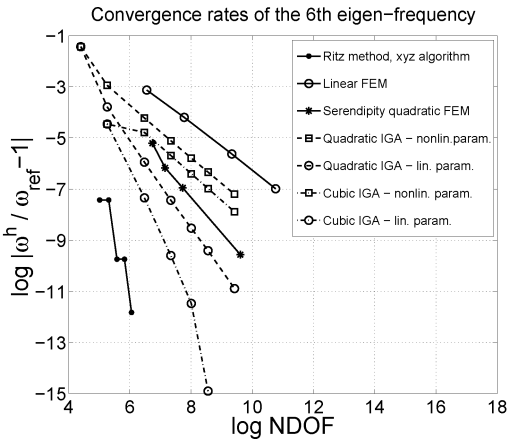

Fig.5: Convergence rates for the sixth non-zero frequency

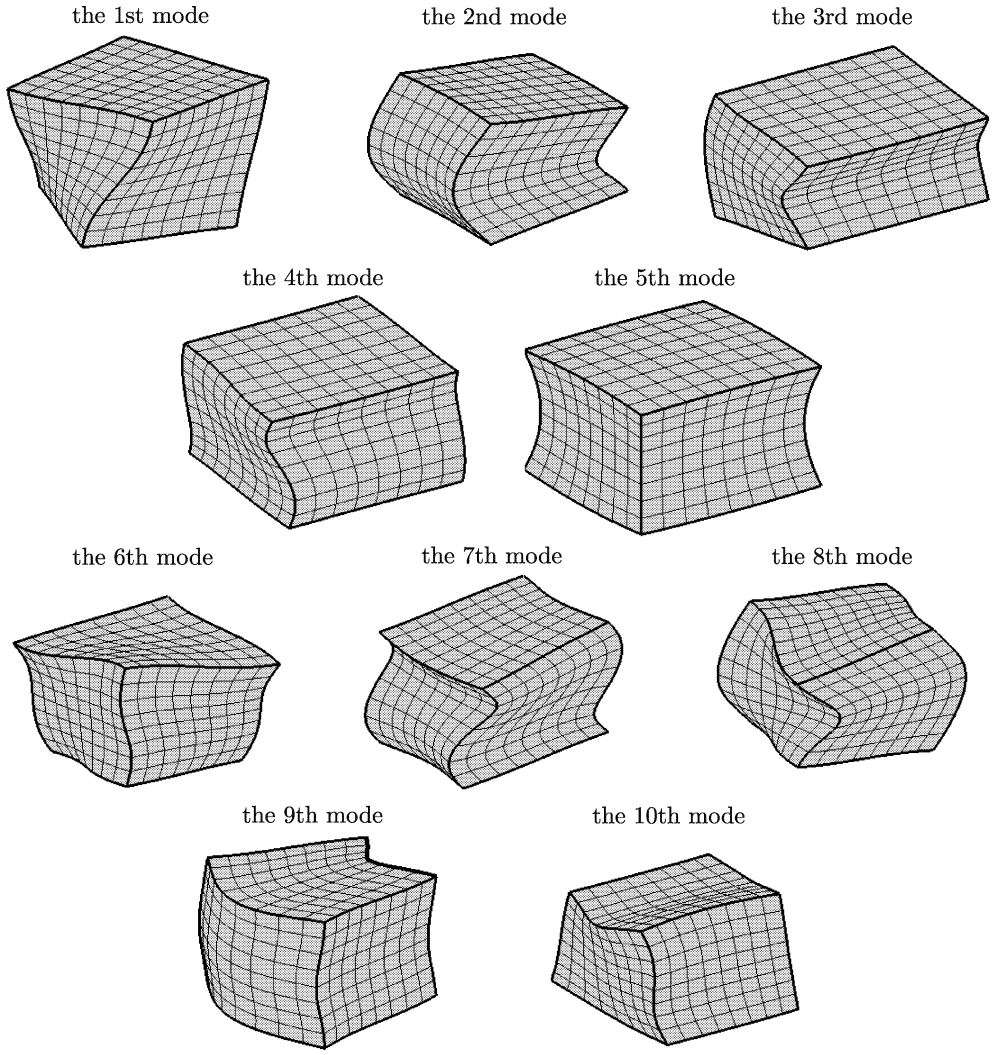

Fig.6: The first ten non-zero eigen-modes of an elastic block made of glass

The first twenty non-zero eigen-frequencies computed for comparable number of degrees of freedom (*NDOF*) is presented in Tab. 1. Results of all applied numerical methods are near experimental data, see Tab. 1. All used methods converge but with different convergence rates. The accuracy and convergence rates are presented and compared for IGA, classical FEM and Ritz method in Figs. 4 and 5. In Fig. 4 convergence rates of the first non-zero eigen-frequency are depicted and the convergence rates of the sixth non-zero eigen-frequency are shown in the Fig. 5. These graphs depict the dependence of relative errors in eigen-frequency $|\omega^h/\omega_{\text{ref}} - 1|$ on number of degrees of freedom of problem (*NDOF*). The reference values of eigen-frequencies ω_{ref} were token from the FEM computation on the mesh density 20×20×20 of quadratic serendipity elements. The division 20×20×20 corresponds to the solution accuracy 10^{-6} [6]. The convergence rate of linear and higher-order FEM is in agreement with the theoretical prediction published in [20], where the convergence rate increases with polynomial order. The convergence rate for IGA strategy can be radically

improved by the linear parameterization given by the Greville abscissa. This effect is obviously demonstrated for cubic IGA convergence rates in Figs. 4 and 5. Certainly, the highest convergence rate was observed for the Rayleigh-Ritz method with high order of polynomials (ten and more).

For illustration, the first ten non-zero eigen-modes of eigen-vibration of an investigated glass block are demonstrated in Fig. 6. For example, the first mode belongs to torsional mode with the axis corresponding to the direction with the maximal length of the block. Further, the second mode is the bending mode along the direction of the middle value of block dimensions.

5. Conclusion

In this paper, the spline finite element method was tested in the eigen-vibration problem of a glass block specimen. It was shown, that the IGA computational strategy is suitable for the determination of eigen-frequencies of elastic bodies. The convergence rate is increasing with order of spline and the convergence rate can be improved by the linear parameterization by the Greville abscissa. On the basis of presented results, the IGA concept has a potential to be employed in high performance and accurate analysis of elastodynamics problems.

On the other side, the cost of the IGA modal analysis is risen with increasing of spline order for constant number of control points due to higher order of continuity of basis functions and their large support. For that reason, the number of non-zero components of mass matrix and stiffness matrix grow up and then these sparse matrices are more filled. In practise, the evaluation of local matrices and principally the assembling process take more time and operations. Therefore these operations play the main role in the IGA analysis of two- and three-dimensional problems [28]. The way, how this disadvantage of the IGA approach could be liquidated, is the improving the numerical integration of mass and stiffness matrices by a more efficient quadrature scheme for spline functions then the Gauss-Legendre quadrature formulae. Furthermore, the total computational times of eigen-value problem are comparable for the same degrees of freedom independently on order of splines, because the degrees of freedoms are not changed. In the future, the performance and accurate analysis of eigen-vibration by the IGA strategy will be realized for simple geometrical specimens like cylinders, spheres, potato shapes and, most especially, for arbitrarily shaped samples.

Acknowledgement

This work was supported by the grant projects GPP101/10/P376 and GAP101/12/2315 under AV0Z20760514.

References

[1] Cottrell J.A., Hughes T.J.R., Bazilevs Y.: Isogeometric Analysis: Toward Integration of CAD and FEA, John Wiley & Sons, New York 2009

[2] Cottrell J.A., Reali A., Bazilevs Y., Hughes T.J.R.: Isogeometric analysis of structural vibrations, Comput. Methods Appl. Mech. Engrg. 195 (2006) 5257–5296

[3] Hughes T.J.R., Reali A., Sangalli G.: Duality and unified analysis of discrete approximations in structural dynamics and wave propagation: Comparison of p-method finite Elements with k-method NURBS, Comput. Methods Appl. Mech. Engrg. 197 (2008) 4104–4124

[4] Schumaker L.: Spline Functions: Basic Theory, Cambridge Mathematical Library, Cambridge University Press, Cambridge, 2007

[5] Schoenberg I.J.: Contributions to the problem of approximation of equidistant data by analytic functions, Quart. Appl. Math. 4 (1946) 45–99 and 112–141
[6] Plešek J., Kolman, R. Landa, M.: Using finite element method for the determination of elastic moduli by resonant ultrasound spectroscopy, Journal of the Acoustical Society of America 116(1) (2004) 282–287
[7] Maynard J.: Resonant Ultrasound Spectroscopy, Phys. Today 49 (1996) 26–31
[8] Migliori A., Sarrao J.L.: Resonant Ultrasound Spectroscopy: Applications to Physics, Materials Measurements, and Non-Destructive Evaluation, John Wiley & Sons, INC., New York, 1997
[9] Love A.E.H.: A Treatise on the Mathematical Theory of Elasticity, Dover Publications, New York, the fourth edition, 1944
[10] Timoshenko S.: Vibration Problems In Engineering, McGraw Hill, third Edition edition, 1961
[11] Holland R.: Resonant properties of piezoelectric ceramic rectangular parellelepipeds, Journal of the Acoustical Society of America 43 (1968) 988–997
[12] Demarest H.H.: Cube resonance method to determine the elastic constants of solids, J. Acoust. Soc. Am. 49 (1971) 768–775
[13] Ohno I.: Free vibration of a rectangular parallelepiped crystal and its application to determination of elastic constants of orthorhombic crystals, J. Phys. Earth. 24 (1976) 355–379
[14] Liu G., Maynard J.D.: Measuring elastic constants of arbitrarily shaped samples using resonant ultrasound spectroscopy, J. Acoust. Soc. Am. 131 (2012) 2068–2078
[15] Visscher W.M., Migliori A., Bell T.M., Reinert R.A.: On the normal modes of free vibration of inhomogeneous and anisotropic elastic objects, Journal of the Acoustical Society of America 90 (1991) 2154–2162.
[16] Piegl L., Tiller W.: The NURBS book, Springer-Verlag, 1997
[17] Kolsky H.: Stress wave in solids, Dover Publications, New York, 1963
[18] Achenbach J.D.: Wave Propagation in Elastic Solids, North-Holland Publishing Comp., American Elsevier Publishing Comp., Inc., 1973, New York
[19] Hughes T.J.R.: The Finite element method: Linear and dynamic finite element analysis, Prentice-Hall, Englewood Cliffs, 1983, New York
[20] Strang G., Fix G.: An Analysis of the Finite Element Method, 2nd edition, Wellesley-Cambridge Press, 2008, Wellesley
[21] Szabo B., Babuška I.: Finite Element Analysis, John Wiley & Sons, INC., 1997, New York
[22] Papadakis E.P.: The Measurement of Ultrasonic Velocity, The Measurement of Ultrasonic Attenuation, Physical Acoustics 19 (1990) 1113–1115
[23] PMD, FEM program, Vamet s.r.o., version f77.10, 2011
[24] Migliori A., Lei M., Schwarz R.: Program RPR, Version 2.02, 1998
[25] Greville T.N.E.: On the normalization of the B-splines and the location of the nodes for the case of unequally spaced knots, Inequalities, ed. Shiska O. Academic Press, 1967, New York
[26] Kolman R., Plešek J., Okrouhlík M., Gabriel D.: Dispersion errors of B-spline based finite element method in one-dimensional elastic wave propagation, In: Computational Methods in Structural Dynamics and Earthquake Engineering ECCOMAS 2011, ed. Papadrakakis M., et al., Corfu, Greece, 2011, 1–12
[27] Matlab, R2011a, MathWorks, 2011
[28] Collier N., Pardo D., Dalcin L., Paszynski M., Calo V.M.: The cost of continuity : A study of the performance of isogeometric finite elements using direct solvers, Comput. Methods Appl. Mech. Engrg. 213–216 (2012) 353–361

Received in editor's office: April 15, 2012
Approved for publishing: June 21, 2012